Camera based Identification and Control of the Waelz Process

Jörg Matthes, Patrick Waibel, Hubert B. Keller and Lutz Gröll
Institute for Applied Computer Science, Karlsruhe Institute of Technology, Hermann-von-Helmholtz-Platz 1, 76344 Eggenstein-Leopoldshafen, Germany

Keywords: Model Identification, Process Control, Infrared Camera, Image Processing, Rotary Kiln, Waelz Process.

Abstract: The Waelz process is the most common technique for the pyro-metallurgical treatment of zinc-bearing residues using a rotary kiln. However, this process will only result in a good zinc recovery, if the temperature of the material (slag) within the kiln is controlled at specific optimal setpoints depending on the material mixture. Until now, slag temperature measurement is carried out by pyrometers which give only pointwise information that can be disturbed by cold slag lumps. Additionally, the temperature control is performed only manually by operators, who have to adapt the amount of process air frequently to keep the process stable at the desired setpoints. In this paper an infrared-camera based measurement of the slag temperature using image processing techniques is presented. Based on that temperature measurement a process model is conducted. Its parameters are estimated by a model-output-error based process identification. The process model is used for the tuning of parameters of an automatic closed loop control. Finally, results from an industrial application of the new camera based slag temperature control are given.

1 INTRODUCTION

Pyro-metallurgical processes like the Waelz kiln process are the technologies most frequently applied worldwide for the recycling of dusty steel mill residues and in particular of EAF (electric arc furnace) dust. The pyro-metallurgical process is characterized by the volatilization of non-ferrous metals like zinc, lead, and cadmium from an oxidized solid mixture through reduction by coke or coal. Concurrently, ferrous oxides are also reduced (Rütten, 2006).

The major component of the Waelz process is the Waelz kiln (Figure 1). It is a rotary kiln (Boateng, 2015) operated counter currently at a rotational speed of ≈1rpm and a slope of 2 to 3 %. The air enters the kiln at the slag discharge end. The solid charge entering at the feed end is first dried and then heated up (temperature ϑ_1) until the reaction starts (temperature ϑ_2). The maximum temperature of the slag reaches about 1250 °C. Under normal operation conditions, the process does not require additional heating; it is auto-thermal.

At about 800 °C, the reduction of the zinc oxide and iron oxide starts. Thus, the zinc volatilizes into the gas phase of the kiln. Here, it is reoxidized and transported as solid dust together with the counter current air flow into a dust chamber.

Some plants additionally make use of the so-called SDHL technique (Saage et al., 2002). Using this technique, supplemental air, so called process air, is added to the slag at the end of the kiln via an air lance in order to reoxidize the metallic iron. The emerging heat can be used for a reduction of the amount of coal needed. Additionally, the process air u_{air} is used as actuating variable to control the slag temperature ϑ_3 at the end of the kiln.

The slag temperature in the kiln has to be controlled in order to achieve an optimum zinc recovery. The temperatures should be high enough to reduce the zinc completely. If the temperature is too high, the material agglutinates and the surface area of the material is reduced. This prevents the zinc from reduction and lowers the zinc recovery. However, the optimum temperatures are no constant values, but depend on the properties of the raw material. Since the raw material is a waste product, these properties may vary. Consequently, the optimum setpoint values for the slag temperature must be adapted frequently by experienced operators, who observe the behavior of the material (slag) at the end of the kiln and adapt the setpoints manually.

In this paper, a custom-built infrared camera together with an appropriate image processing system will be described. It can be used for improving observation, temperature measurement, and control of the Waelz kiln. Based on the camera based tempera-

Matthes, J., Waibel, P., Keller, H. and Gröll, L.
Camera based Identification and Control of the Waelz Process.
DOI: 10.5220/0005957402910298
In *Proceedings of the 13th International Conference on Informatics in Control, Automation and Robotics (ICINCO 2016) - Volume 1*, pages 291-298
ISBN: 978-989-758-198-4

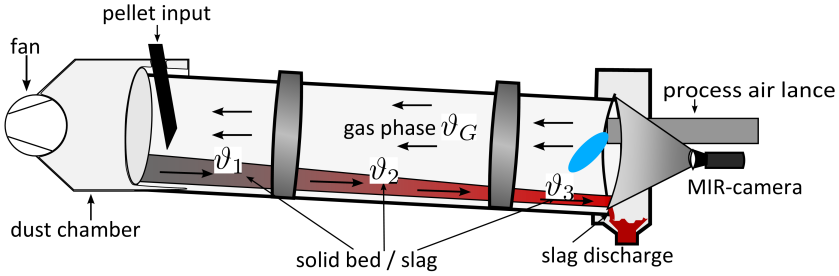

Figure 1: Scheme of a Waelz kiln for zinc recycling with SDHL-process air lance and infrared camera for slag temperature measurement.

ture measurement a simplified process model is presented. Its parameters are estimated by minimizing the model-output-error. The process model is then used for the controller tuning for an automatic closed loop control. Finally, results from the industrial application of the new camera based slag temperature control system are given.

2 CAMERA BASED TEMPERATURE MEASUREMENT

Unfortunately, the view into the kiln in the visible spectral range is poor, which may lead to a false rating of the current behavior of the slag as shown in Figure 2 (left). For this reason, a custom-built IR camera (PYROINC 320F from DIAS-INFRARED, uncooled micro bolometer system) with a spectral filter at 3.9 µm is used for the observation of the Waelz kiln. In this spectral band, all relevant gas components are nearly transparent and negative influence of small particles (here, zinc oxide) in the kiln's atmosphere on the transmissivity is reduced. Figure 2 (right) shows such an IR camera image of the end of the Waelz kiln. Compared to the VIS camera, the IR camera allows for a deep insight into the kiln.

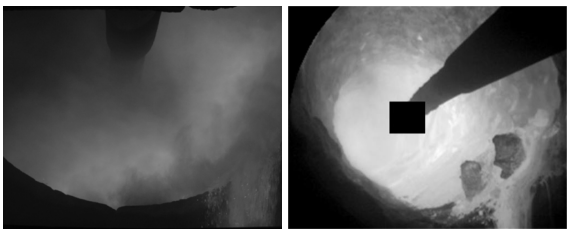

Figure 2: Comparison of a standard CCD camera image in the visible spectral range (left) and of an IR camera with a spectral filter at 3.9 µm at the end of the Waelz kiln (right) (Tip of air lance is covered on legal grounds).

Another problem is the measurement of the slag temperature. Until now, pyrometers are used, which measure a single spot of the slag only. Cold lumps in the slag at this spot may result in significant measurement errors of the slag temperature as demonstrated in Figure 3. The resulting temperature signal drops in case of cold lumps and gives a wrong information about the slag temperature for the plant operator. If an IR camera system is used, the whole slag region can be used for calculating the mean slag temperature. Additionally, an image processing algorithm to detect cold lumps allows to omit the cold lumps for the mean temperature calculation. Thus, a much more reliable measurement of the slag temperature is possible based on the IR camera system. This also improves the quality of the slag temperature control.

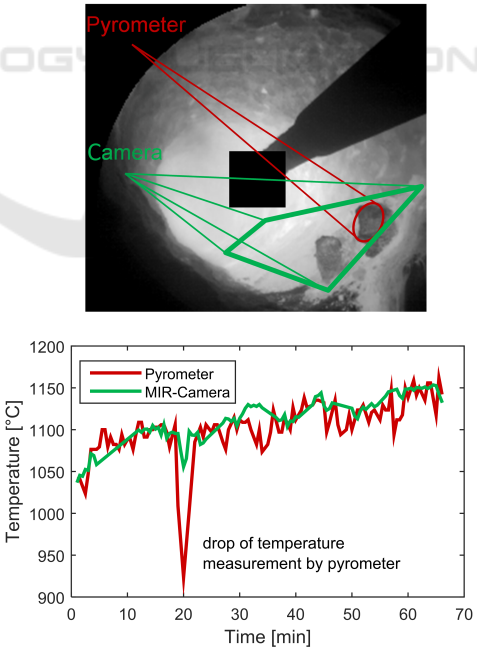

Figure 3: Slag temperature measurement with pyrometer compared to IR camera.

3 IMAGE PROCESSING

Deep insight into the Waelz kiln with the IR camera is very useful for the manual inspection of the process. Control room operators can early detect relevant changes in the process. However, application of an IR camera is aimed at integrating camera information in the closed loop control of the kiln. For this purpose, a reliable image processing system is required, which extracts process-relevant information from the IR images. This information must be expressed in suitable process parameters which describe the current state of the process and the slag and can be used directly in the process control system. Figure 4 gives an overview of the structure of the image processing system. The single steps will be explained below.

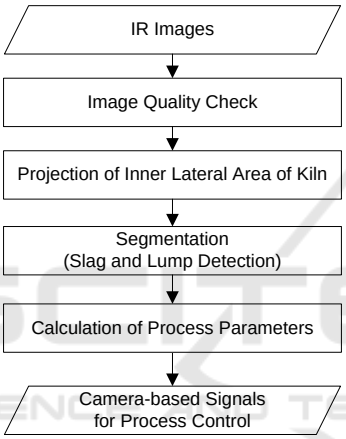

Figure 4: Structure of the image processing system.

Due to failures of the camera system or temporarily heavy dust load in the kiln's atmosphere, the image quality may be too low for a reliable calculation of process parameters from the IR images. Since the camera and image processing system are part of the closed loop control, such failures have to be detected automatically and reported to the process control system. Accordingly, the first step of image processing is the determination of the image quality. It is based on plausibility checks of temperature and contrast ranges in the image. Only if these checks are passed successfully, does image processing proceed.

Then, the geometric projection of the inner lateral area of the kiln is calculated. The inner lateral area as well as the solid bed area become a rectangle. It allows for the equal-area calculation of temperatures and other properties of the kiln's interior. The original infrared image and the projection of the inner lateral area of the kiln are depicted in Figure 5.

Since the solid bed (slag) properties are of special interest to the Waelz process, the next task is to detect

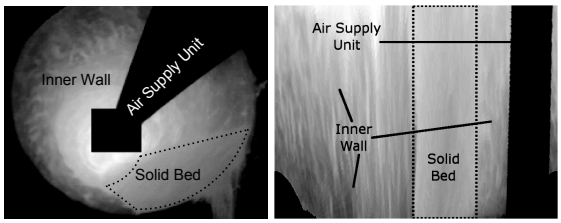

Figure 5: Original infrared image and projection of inner lateral area of the kiln.

the solid bed region in the IR image, i. e. to segment the image into the solid bed region and the remainder (inner wall of kiln) (Waibel et al., 2010). A straightforward way to detect the solid bed region is to use the temperature difference between the solid bed and the inner wall of the kiln. However, there are process situations with marginal temperature differences only, which could cause a wrong segmentation result. For such situations, a motion-based image segmentation algorithm was developed (Waibel et al., 2010). It analyzes the motion (the so-called optical flow (Brox et al., 2004)) in x-direction in the projected image.

In some process situations, cold lumps in the slag may distort the calculation of temperature profiles of the solid bed. For this reason, image processing performs an automatic lump detection which is based on the difference between the mean solid bed temperature and the lump temperature. The size and number of the detected lumps are calculated as additional process parameters. For further calculations, e.g. for the calculation of th control variable mean solid bed/slag temperature ϑ_3, the detected lump regions are omitted, which improves the reliability of the solid bed temperature measurement compared to a pyrometer (see Figure 3). Additionally, information about the rheological behavior of the slag like repose and filling angle can be extracted from the IR images (Matthes et al., 2011),(He et al., 2009).

For industrial application, the image processing algorithms are integrated into the software tool INSPECT PRO CONTROL.

4 CAMERA BASED PROCESS IDENTIFICATION

The basis for a theoretic modeling of rotary kiln processes are the balance equations for mass, energy, impulse and materials. They form a system of partial differential equations (Boateng, 2015). For a numerical solution they can be discretized in space and thus transformed into a large system of coupled ordinary differential equations. The large number of chemi-

cal and physical parameters contained in this system (here > 100) are mostly unknown. An experimental identification of this large number of parameters is not feasible, since only little measurement information can be obtained from the inner of the rotary kiln. Thus, the complex material and heat transfer processes as well as the chemical reactions within the rotary kiln prevent a straight theoretic modeling of the zinc recycling process.

For the design of a closed loop control for the slag temperature ϑ_3 at the end section of the rotary kiln (see Figure 1) a simplified process model is sufficient. The simplified process model should only reflect the control relevant dynamics of the system and contain only a small number of parameters. Here, the structure of such a simplified model is deduced from a qualitative theoretic process analysis. Then, the parameters are identified based on experiments at the industrial rotary kiln.

4.1 Model Structure

The input signal of the simplified model is the process air u_{air} normalized to the range of 0-100%. The output of the model is the slag temperature ϑ_3 at the end of the rotary kiln (see Figure 1), which is the control variable and is measured by means of the IR-camera system as described in the previous sections. The simplified model only regards changes Δu_{air} and $\Delta\vartheta_3$ with respect to the current operating point $(u_{air,e}, \vartheta_{3,e})$. To have a better relation to the actual rotary kiln process, the absolute values $\Delta u_{air} + u_{air,e}$ and $\Delta\vartheta_3 + \vartheta_{3,e}$ are depicted in the diagrams. For the sake of readability from now on Δ is omitted for all signals.

Figure 6 shows an experimental step response of the system starting from operating point ($u_{air,e} = 53\%, \vartheta_{3,e} = 1125\,^{\circ}\mathrm{C}$). Here the process air u_{air} was increased from 53% to 73% (i. e. by 20 pp) at minute 19. The increase of process air leads to a rapid decrease of the slag temperature ϑ_3 from approx. 1125 °C to 1090 °C due to the cooling effect of the increased process air. Parallely, the increase of process air causes an increase in the exothermic oxidation of iron in the slag, which leads to a slow increase in resulting heating power and thus to an increase of the slag temperature ϑ_3 up to 1200 °C. This is a typical behavior of combustion processes where the increase of a fuel component (here air) leads to a short-term decrease of temperature before the exothermic combustion leads to a long-term temperature increase. In control theory this is known as all-pass behavior.

The left part of the signal flow diagram in Figure 7 represents the described behavior between the process

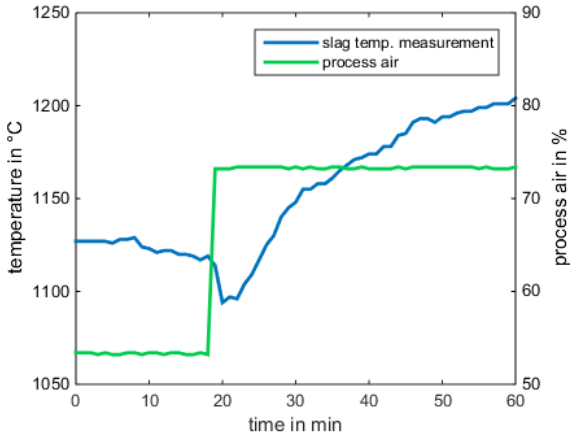

Figure 6: Step response of the slag temperature when process air changes.

air u_{air} and the heating power P_{heat}, that results from the cooling and the exothermic reaction. The PT1-element with a small time constant $T_{air} = 1\text{min}$ covers the already known dynamics of the air lance, since the change of the setpoint for u_{air} does not change the actual process air u'_{air} immediately. The short-term cooling effect (P_{cool}) is only significant when the process air u_{air} is increased. For this reason, in the model the sign of $\dot{u}_{air}$ is evaluated. Here the DT1-element with time constants T_{cool} and T'_{cool} characterizes the dynamic of the short-term cooling effect. The gain K_{oxid} represents the relation between process air and heating power due to the Fe-oxidation.

The long-term increase of heating power due to an increase in process air leads to a long-term increase of slag temperature ϑ_3. In the model this is described by an PT1-element with time constant T_3 and gain K_{3P} shown in the right part of Figure 7. The increase of ϑ_3 causes an increase of the gas phase temperature ϑ_G described by a PT1-element with time constant T_G and gain K_{G3}. Since the gas moves in the opposite direction to the slag (see Figure 1), it is heating the slag in zone 2 (ϑ_2). The dynamics of the heat transfer is expressed again by a PT1-element with time constant T_2 and gain K_{2G}. Changes in the slag temperature ϑ_2 influence the slag temperature ϑ_3 due to heat and mass transfer. This effect is covered in the model by an additional virtual heating power $K_{32} \cdot \vartheta_2$ proportional to temperature ϑ_2.

From Figure 7 the model can be expressed with the following equations.

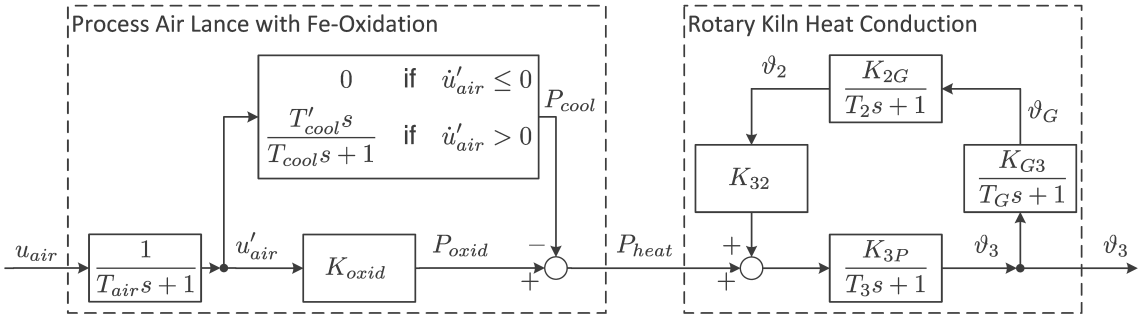

Figure 7: Signal flow diagram of the simplified model for slag temperature in the rotary kiln.

Process air lance and the Fe-oxidation:

$$T_{air}\dot{u}'_{air} = -u'_{air} + u_{air} \tag{1}$$

$$P_{cool} = 0 \qquad \text{if } \dot{u}'_{air} \le 0 \tag{2}$$

$$T_{cool}\dot{P}_{cool} = -P_{cool} + T'_{cool}\dot{u}'_{air} \qquad \text{if } \dot{u}'_{air} > 0 \tag{3}$$

$$P_{oxid} = K_{oxid}u'_{air} \tag{4}$$

$$P_{heat} = P_{oxid} - P_{cool} \tag{5}$$

Heating and heat transfer within the rotary kiln:

$$T_3\dot{\vartheta}_3 = -\vartheta_3 + K_{3P}(K_{32}\vartheta_2 + P_{heat}) \tag{6}$$

$$T_G\dot{\vartheta}_G = -\vartheta_G + K_{G3}\vartheta_3 \tag{7}$$

$$T_2\dot{\vartheta}_2 = -\vartheta_2 + K_{2G}\vartheta_G \tag{8}$$

4.2 Parameter Estimation

The simplified model presented in the previous section contains only 10 parameters

$$\theta = \left(T'_{cool}, T_{cool}, K_{oxid}, T_3, K_{32}, K_{3P}, T_G, K_{G3}, T_2, K_{2G}\right)^T \tag{9}$$

that have to be estimated based on experimental data.

In Figure 8 the results of three experiments at the industrial rotary kiln for zinc recycling are shown for the temperature ϑ_3. Each experiment lasts 240 minutes and starts in a slightly different operating point of the plant. In the experiments the process air u_{air} was varied to investigate the dynamic behavior of the rotary kiln. It should be mentioned, that open loop experiments at the industrial plant are very expensive, since the optimal operating point is left for hours. Even after each 4-hour-experiment it took a couple of hours to reach an optimal static state of the plant again. For this reason, only 3 experiments could be performed, which are the basis for the parameter estimation.

By numerical simulation (e.g. using Matlab) for a given estimate of the parameter vector $\hat{\theta}$ the model can be used to calculate the signal $\hat{\vartheta}_3(t;n,\hat{\theta})$ for each experiment $n = 1,\ldots,3$ using the corresponding operating point and input signal $u_{air}(t;n)$. When the same

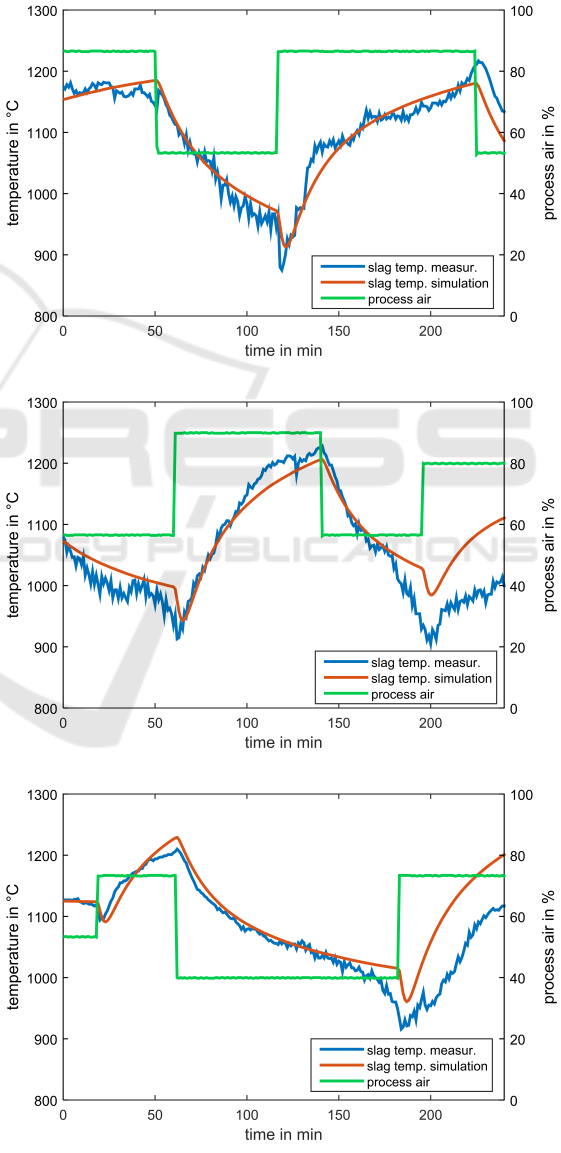

Figure 8: Experimental results for slag temperature ϑ_3 (blue) at industrial rotary kiln resulting from variations in process air u_{air} (green) used for parameter identification and simulation results (red) with optimal parameters $\hat{\theta}_{opt}$.

input signals are used for the experiments and the numerical simulation, then, with a perfect estimate $\hat{\theta}$ the measured output signal $\vartheta_3(t;n)$ from experiment n would be the same as the output signal $\hat{\vartheta}_3(t;n,\hat{\theta})$ from the numerical simulation for each t.

Due to the simplified model structure and disturbances in the experimental data there will be a model output error

$$e_M(t;n,\hat{\theta}) = \vartheta_3(t;n) - \hat{\vartheta}_3(t;n,\hat{\theta}) \qquad (10)$$

Here, the parameter vector $\hat{\theta}_{opt}$ is searched for, that minimizes the integral squared model output error over all three experiments

$$\underset{\hat{\theta}}{\text{minimize}} \quad \sum_{n=1}^{3} \int_{0\text{min}}^{240\text{min}} e_M(t;n,\hat{\theta})\mathrm{d}t \qquad (11)$$

Minimizing the model output error (also known as simulation error) to find the plant parameters has a number of advantages.

First, the model output error approach can be applied to any kind of model structure (e. g. nonlinear) as long as a numerical simulation of the model can be performed.

Second, although for linear models, an equation error based least squares minimization is computationally faster, it is much more sensitive to measurement noise. The output error approach is more robust and gives the maximum-likelihood estimate for the parameters. Thus, for an offline parameter estimation, where computational speed is not important, minimizing the output error is the best choice.

The search for the optimal parameters is performed by a simplex search method (Lagarias et al., 1998). It starts at an initial value $\hat{\theta}_0$ and may only give a local solution. For that reason different (technical reasonable) initial values $\hat{\theta}_0$ are applied in order to find the global solution.

As a result, the minimal integral squared output error is obtained for the following parameter values:

$K_{oxid} = 0.4$ kW/pp	$T_{cool} = 2$ min
$T'_{cool} = 12$ kW min/pp	$T_3 = 20$ min
$K_{32} = 0.9$ kW/K	$K_{3P} = 1.0$ K/kW
$T_G = 1$ min	$K_{G3} = 1.0$
$T_2 = 30$ min	$K_{2G} = 0.5$

As expected by process experts, the time constants $T_2 = 30$ min and $T_3 = 20$ min for the slag temperatures ϑ_2 and ϑ_3 are the dominant time constants of the process. The cooling of the slag surface due to increased process air and the change of gas phase temperature ϑ_G are considerably faster.

4.3 Model Validation

For the validation of the model and its parameters the results of numerical simulations of the model are compared with the experiments in Figure 8. For the simulation, only the operating point at $t = 0$ and the input signal $u_{air}(t)$ are known.

The first experiment shows a very good match of the simulated temperature with the measured temperature over the whole 240 min. In the second and third experiment only after 200 min a slight deviation can be observed.

This means, that the model can be used to forecast the slag temperature ϑ_3 for more than three hours and is thus suitable for a model based controller design.

5 CAMERA BASED SLAG TEMPERATURE CONTROL

Using the process model from the previous section the controller is designed and tested by numerical simulations of the closed loop. Then, results from the industrial application of the new camera based controller are presented.

5.1 Model based Controller Design

To control the slag temperature ϑ_3 at its desired setpoint $\vartheta_{3,d}$ a PID-controller

$$u_{air} = K_P e(t) + \frac{1}{T_N}\int_0^t e(\tau)\mathrm{d}\tau + T_V \dot{e}(t) \qquad (12)$$

with control error

$$e(t) = \vartheta_{3,d}(t) - \vartheta_3(t) \qquad (13)$$

is applied. Here a PID-controller is the first choice, because it is effective, widely accepted in the industrial environment and can easily be integrated into existing process control systems. Since the actuating variable process air u_{air} is limited to $0\ldots100\%$ an integration wind-up could occure. For that reason, an integrator stop is implemented as anti-windup method (Åström and Hägglund, 2006).

The controller parameters K_P, T_N, T_V are tuned on the basis of the numerical process model described in Section 4.

Figure 9 shows the simulated closed loop behavior with controller parameters $K_P = 1, T_N = 20$ min, $T_V = 10$ min. Starting from operating point 900 °C, the setpoint for the desired temperature is increased at $t = 30$ min to 1000 °C. The slag temperature drops slightly due to the all-pass-behavior and then slowly

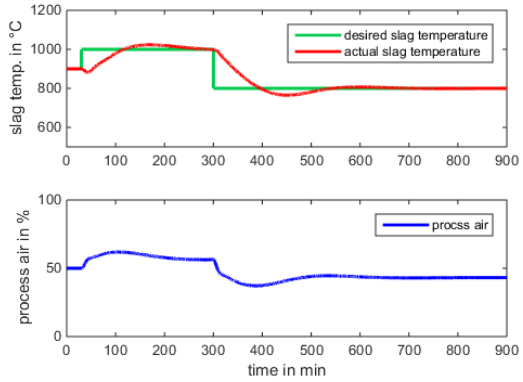

Figure 9: Simulated closed loop behavior with controller parameters $K_P = 1, T_N = 20$ min, $T_V = 10$ min.

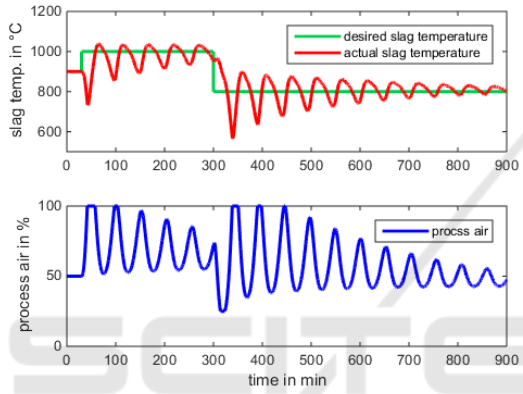

Figure 10: Simulated closed loop behavior with controller parameters $K_P = 10, T_N = 20$ min, $T_V = 10$ min.

follows the setpoint change and reaches the new setpoint after approx. 90 min. If the setpoint is changed to 800 °C at $t = 300$ min again the slag temperature slowly follows and reaches the new setpoint after approx. 90 min. With a slight overshoot a constant slag temperature at the desired value is reached after approx. 200 min at $t \approx 500$ min. In the lower part of Figure 9 the corresponding course of the process air is plotted.

The undesired slow convergence of the slag temperature to new setpoints can be improved by increasing the controller gain K_P. Figure 10 shows the simulated closed loop behavior with controller parameters $K_P = 10, T_N = 20$ min, $T_V = 10$ min. When the setpoint is increased at $t = 30$ min the controller yields a fast increase in process air. Due to the all-pass-behavior of the system, the slag temperature drops and thus, the control error e grows even more, which yields to a further increase of u_{air} until it reaches its limit at 100%. As a result the control variable ϑ_3 as well as the actuating variable u_{air} start oscillating unacceptably.

The example shows, that due to the all-pass-behavior a careful tuning of the controller parameters is necessary. A trade-off between fast convergence of slag temperature to new setpoints and stability has to be found. This holds also for the remaining controller parameters T_N and T_V.

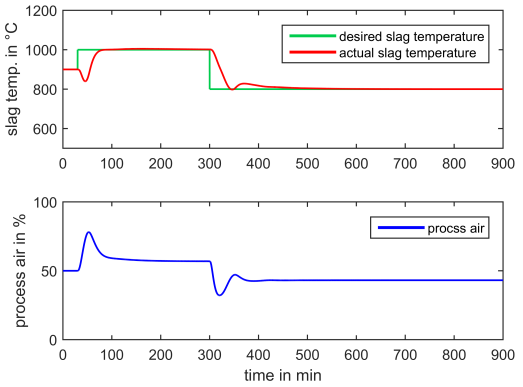

Figure 11: Simulated closed loop behavior with controller parameters $K_P = 4, T_N = 20$ min, $T_V = 10$ min.

Such a trade-off is obtained with controller parameters $K_P = 4, T_N = 20$ min, $T_V = 10$ min as depicted in Figure 11. With these controller parameter values a sufficient fast convergence of the slag temperature to new setpoints is provided and oscillations are prevented.

5.2 Industrial Controller Validation

The PID-controller described in the previous section was implemented in a time-discrete form and integrated into the INSPECT PRO CONTROL software. A new value for the controller output u_{air} is transfered to the process control system every 5 sec.

So far, the process air u_{air} has been manipulated manually by an experienced operator to control the slag temperature ϑ_3. Now, the operator can change from manual to automatic control mode to apply the controller calculated process air to the plant. When switching from manual to automatic control mode the integrator of the PID-controller is set to the last manually set process air value to obtain a shock-free behavior (process air value does not jump).

To compare the quality of manual control by experienced operators with the new automatic control, in Figure 12 two examples are given. Each figure shows the course of the desired temperature $\vartheta_{3,d}$, the camera-based measured slag temperature ϑ_3 and the process air u_{air} for approx. 8 hours. In each case the first 4 hours are in manual control mode followed by 4 hours of automatic control mode.

In manual control mode the process air is only changed in time intervals of at least 10 min. In auto-

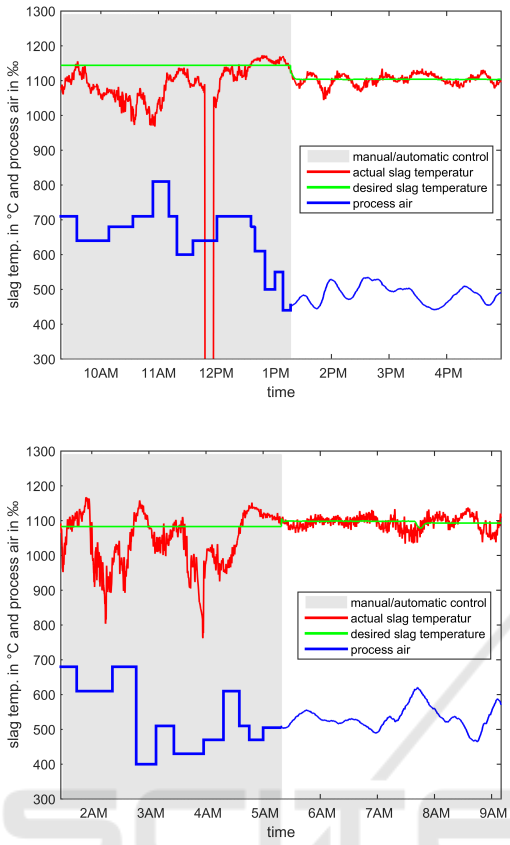

Figure 12: Comparison of manual control (first 4 hours) and automatic control using the new camera based controller (following 4 hours) at two different days.

matic mode a quasi continuous adaptation of process air is performed every 5 sec. At day 1 at 12 pm the camera was removed for about 10 min which leads to missing temperature measurements.

For both days the automatic control yields a significant smaller variation of the slag temperature around its setpoint. Thus a higher process efficiency is obtained using the new camera based controller.

6 CONCLUSION

In this paper a new model based closed loop slag temperature control for the Waelz process is presented. It is based on an IR camera measurement of the slag temperature using image processing techniques. With this reliable temperature measurement, a simplified process model is conducted. It describes the dynamic relation between process air and slag temperature. The model parameters are estimated by a model-output-error based process identification. The model allows for a good slag temperature prediction for more than three hours. Additionally, the model reveals an all-pass-behavior of the slag temperature. Subsequently, it is used for tuning the parameters of a PID automatic closed loop control. It shows, that due to the all-pass-behavior a careful tuning of the controller parameters is necessary. The parameters found are a trade-off between fast convergence of slag temperature to new setpoints and stability, i. e. preventing oscillations. Finally, results from an industrial application of the new camera based slag temperature control are given, which show a significant improvement compared to the manual control. The complete camera based control system presented here has been implemented successfully at an industrial plant. Future works comprise a deeper analysis of the process structure and the investigation of model predictive control approaches to further improve the Waelz process.

REFERENCES

Åström, K. and Hägglund, T. (2006). *Advanced PID Control*. ISA-The Instrumentation, Systems, and Automation Society.

Boateng, A. (2015). *Rotary Kilns: Transport Phenomena and Transport Processes*. Elsevier Science.

Brox, T., Bruhn, A., Papenberg, N., and Weickert, J. (2004). High accuracy optical flow estimation based on a theory for warping. In *Computer Vision - ECCV 2004*, volume 3024 of *Lecture Notes in Computer Science*, pages 25–36. Springer.

He, M., Zhang, J., and Liu, X. (2009). Determination of the repose angle of stuff in rotary kiln based on imaging processing. In *9th International Conference on Electronic Measurement & Instruments (ICEMI) 2009*, pages 4–97–4–101.

Lagarias, J. C., Reeds, J. A., Wright, M. H., and Wright, P. E. (1998). Convergence properties of the nelder-mead simplex method in low dimensions. *SIAM Journal of Optimization*, 9:112–147.

Matthes, J., Waibel, P., and Keller, H. B. (2011). A new infrared camera-based technology for the optimization of the waelz process for zinc recycling. *Minerals Engineering*, 24(8):944–949.

Rütten, J. (2006). Application of the waelz technology on resource recycling of steel mill dust. *SEAISI Quarterly (South East Asia Iron and Steel Institute)*, 35:13–19.

Saage, E., Hasche, U., Dittrich, W., and Langbein, D. (2002). Method of utilizing secondary raw materials containing iron, zinc and lead. US Patent 6,494,933.

Waibel, P., Matthes, J., and Keller, H. B. (2010). Segmentation of the solid bed in infrared image sequences of rotary kilns. In *Proceedings of the 7th International Conference on Informatics in Control, Automation and Robotics (ICINCO)*, pages 217–220.